Phys. Status Solidi B **247**, Nos. 11–12, 2847–2850 (2010) / **DOI** 10.1002/pssb.201000294

physica status solidi b
www.pss-b.com
basic solid state physics

Chirality dependence of the dielectric constant for the excitonic transition energy of single-wall carbon nanotubes

P. T. Araujo*,[1], A. R. T. Nugraha[2], K. Sato[2], M. S. Dresselhaus[3], R. Saito[2], and A. Jorio[1]

[1] Departamento de Física, Universidade Federal de Minas Gerais, Belo Horizonte 30123-970, Brazil
[2] Department of Physics, Tohoku University, Sendai 980-8578, Japan
[3] Department of Physics, Massachusetts Institute of Technology, Cambridge, MA 02139-4307, USA

Received 3 May 2010, accepted 10 June 2010
Published online 21 September 2010

Keywords carbon nanotubes, dielectric screening, energy transitions, excitons

* Corresponding author: e-mail pauloata@fisica.ufmg.br, Phone: +55-31-34096610, Fax: +55-31-34095600

Attention has been devoted recently to understand the physics behind the dielectric screening of the carbon nanotube optical transitions (E_{ii}), including how a changing environment changes E_{ii}. It was shown that the environmental screening could be modeled by an effective diameter dependent dielectric constant κ, which takes into account contributions from the single-wall carbon nanotube (SWNT) itself and from the environment surrounding the tube. Here we consider the chiral angle (θ) dependence of κ which improves the previous fitting by only the diameter dependence and we can now see the difference between E_{11}^{M} and E_{22}^{S} by the present treatment. In this work we used the "alcohol-assisted" and the "super-growth" SWNT samples to address this point.

1 Introduction The accurate description of the optical transition energies (E_{ii}) and of the relation between the radial breathing mode frequencies (ω_{RBM}) and the tube diameter (d_t) has attracted a great deal of attention in the field of single wall carbon nanotubes (SWNTs) [1–4]. From the scientific point of view, describing accurately E_{ii} and ω_{RBM} means understanding deeply the relevant physical phenomena, which includes many-body and environmental effects [4–12]. From a practical point of view, when performing optical experiments such as photoluminescence and Raman spectroscopy, E_{ii} and ω_{RBM} give us information to assign the SWNT's structural (n, m) indices. Knowing the (n, m) indices of a SWNT allows scientists in many fields (synthesis, electrical transport, device engineering) to work on the single molecular level with a well-defined structure [13–19]. However, to accurately assign an (n, m) index, it is necessary to know very well the E_{ii} and ω_{RBM} for a standard SWNT, and to understand beyond this, how environmental effects can change such standard properties. While the ω_{RBM}'s behavior when the tube is interacting with some environment is largely understood a complete description of the E_{ii}'s problem is still under development [20, 21]. The state-of-the-art theoretical calculations, which take into account curvature and many-body effects, are still unable to accurately describe the experimentally obtained E_{ii} results [4–12]. The reason for such a mismatch is that E_{ii} strongly depends on the dielectric constant of the SWNT and its environment. As a consequence, lots of different values of E_{ii} have been published in the literature for "similar" samples, urging the need for one unified big picture [13–19, 22]. In this paper, we wish to clarify and discuss some main aspects of finding an appropriate description for the SWNTs dielectric screening and, thereby, describe, within experimental accuracy, all experimental E_{ii}.

2 The d_t dependence of the dielectric constant Recently, we have used the experimental E_{ii} values of many SWNTs assigned from the "super-growth" (SG) and "alcohol-assisted" (AA) samples [13, 20] in order to model and calculate the dielectric constant (κ) [23]. The E_{ii} values can be renormalized in the calculation by explicitly considering the dielectric constant κ in the Coulomb potential energy $V(q)/\varepsilon(q)\kappa$ [24]. Here, κ represents the screening of the e–h (electron–hole) pair by core (1s) and σ electrons (κ_{tube}) and by the surrounding materials (κ_{env}). $\varepsilon(q)$ explicitly gives the polarization function for π-electrons calculated within the random phase approximation (RPA) [7, 25, 26]. To fully account for the observed energy-dependent E_{ii} redshift, we fit the total κ values $((1/\kappa = C_{\rm env}/\kappa_{\rm env} + C_{\rm tube}/\kappa_{\rm tube}))$ [24] to minimize $E_{ii}^{\rm exp} - E_{ii}^{\rm cal}$. Looking at the expression for κ one can conclude that $\kappa_{\rm tube}$ is intrinsic to the SWNT properties and it is not expected to change from tube to tube, while $\kappa_{\rm env}$ depends on the environment. To describe E_{ii} and find a set of κ values have allowed us to establish a semi-empirical relation between κ and $d_{\rm t}$ given by [23],

$$\kappa = C_\kappa \left(\frac{p}{d_{\rm t}}\right)^{1.7}, \tag{1}$$

where, in Ref. [23], $C_\kappa = 0.75$ was found for E_{11}^S, E_{22}^S, and E_{11}^M for the SG SWNTs and $C_\kappa = 1.02$ for the AA SWNTs. For higher transitions, namely E_{33}^S and E_{44}^S, $C_\kappa = 0.49$ was found for both samples. The constant p is defined as 1, 2, 3, 4, and 5 for E_{11}^S, E_{22}^S, E_{11}^M, E_{33}^S, and E_{44}^S, respectively [27]. The $d_{\rm t}$ dependence of κ can be qualitatively understood by considering the amount of the exciton's electric field "feeling" the environment surrounding the SWNT and also by considering the exciton size (which is strongly dependent of $d_{\rm t}$) for each tube and energy transition. The higher energy transitions are described with the same C_κ because the electric field lines for these transitions cannot go much outside the SWNTs and, therefore, they cannot effectively interact with the environment, in contrast to what happens to the lower energy transitions [23].

3 The chirality dependence of the dielectric constant Nowadays the importance of excitons in the SWNTs electronic transitions is very clear from both an experimental and theoretical point of view [4–13]. As shown by Jiang et al. [7], the SWNTs excitonic levels show a considerable dependence on the SWNT chirality, which is shown by the so-called family dependence behavior [4]. As the interaction which maintains the SWNT's excitons stability is essentially Coulombic [4] and, therefore, κ dependent, it is interesting to verify how important it is to correct κ for the SWNT chiral angle (θ). As mentioned above, κ is composed of $\kappa_{\rm tube}$ and $\kappa_{\rm env}$. However, $\kappa_{\rm tube}$ is totally dependent on the SWNTs structure and is also possibly θ dependent. In order to verify such a dependence, a term accounting for the chirality was introduced into Eq. (1) that now reads,

$$\kappa = C_\kappa \left(\frac{p}{d_{\rm t}}\right)^{1.7} + B_p \frac{\cos(3\theta)}{d_{\rm t}^2}, \tag{2}$$

where B_p is weighting the chirality contribution for the different E_{ii}. Our analysis is again directed to the SG and AA samples [13, 20].

Figure 1 shows a plot of κ fitted to the AA (E_{22}^S, E_{11}^M) transitions as a function of $p/d_{\rm t}$. All κ values were obtained and optimized in accordance with the explanation presented in Section 2. In Fig. 1(a) κ has been chiral angle corrected

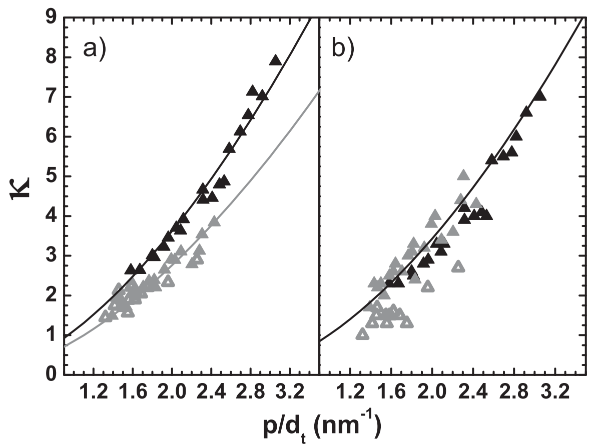

Figure 1 The κ values fitted to the AA E_{11}^M (black triangles) and E_{22}^S (solid/open gray triangles) transitions. Parts (a) and (b) show, respectively, results for κ when the chirality correction is taken into account and when it is not. While the solid gray triangles stand for E_{22}^S type I the open gray triangles stand for E_{22}^S type II. In (a) the black and gray curves are obtained by fitting the data with Eq. (2) and the curve in (b) is given by Eq. (1).

using the second term in Eq. (2) while in Fig. 1(b) it was not. By comparing Figs. 1(a) and (b) it is clear that the chirality correction has improved the κ's evaluation and, of particular importance, the κ fitted to E_{11}^M (black triangles) no longer collapses onto the same curve as those fitted to E_{22}^S (solid/open gray triangles), but rather appears on a curve higher than that for E_{22}^S. This result is quite interesting since the dielectric screening for metallic tubes is more critical because of the presence of free carriers, and this would make them follow different scalings. The same behavior can be observed for the SG κ values, as exhibited in Fig. 2.

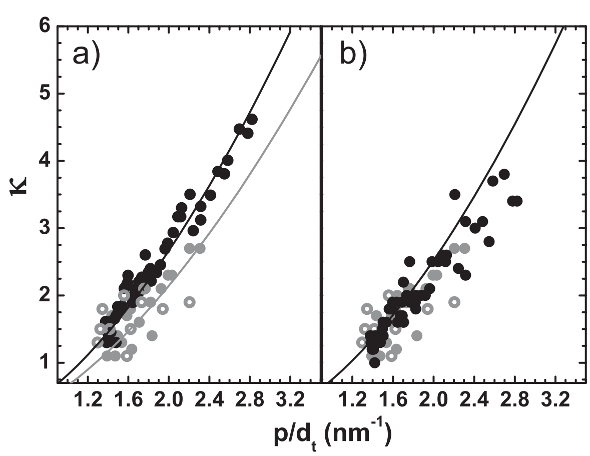

Figure 2 The κ values fitted to the SG E_{11}^M (black bullets) and E_{22}^S (solid/open gray bullets) transitions. Parts (a) and (b) show, respectively, results for κ when the chirality correction is taken into account and when it is not. While the solid gray bullets stand for E_{22}^S type I, the open gray bullets stand for E_{22}^S type II. In (a) the black and gray curves are obtained by fitting the data with Eq. (2), and the curve in (b) is given by Eq. (1).

Table 1 C_κ values found by fitting κ with Eq. (2).

AA's C_κ	SG's C_κ
$C_\kappa^{E_{11}^M} = 0.82$	$C_\kappa^{E_{11}^M} = 1.11$
$C_\kappa^{E_{22}^S} = 0.66$	$C_\kappa^{E_{22}^S} = 0.85$
$C_\kappa^{E_{33,44}^S} = 0.49$	$C_\kappa^{E_{33,44}^S} = 0.49$

Table 2 B_p values found by fitting κ with Eq. (1). In the column's titles, lower(higher) stand for the lower(higher) E_{ii} branches.

AA's B_p lower(higher)	SG's B_p lower(higher)
$B_p^{E_{22}^S} = 1.2(-1.1)$	$B_p^{E_{22}^S} = 0.1(-0.1)$
$B_p^{E_{11}^M} = 1.3$(not measured)	$B_p^{E_{11}^M} = 1.4$(not measured)
$B_p^{E_{33}^S} = 0.95(-0.55)$	$B_p^{E_{33}^S} = 1(-0.2)$
$B_p^{E_{44}^S} =$ not measured(-0.3)	$B_p^{E_{44}^S} =$ not measured(-0.3)

Similarly, in Figs. 2(a) and (b) the κ values are, respectively, corrected and not corrected for the chiral angle κ dependence for the SG SWNTs. Again, the κ values for E_{11}^M transitions (black bullets) appear higher than the values for E_{22}^S and both do not collapse onto the same curves. In both Figs. 1(a) and 2(a) the black and gray solid lines are fittings using Eq. (2). The curves in Figs. 1(b) and 2(b) are given in Ref. [23]. The values for C_κ and B_p are found in Tables 1 and 2, respectively.

Figure 3 shows a plot of κ fitted to the AA and SG (E_{33}^S, E_{44}^S) transitions as a function of p/d_t. Once more, Figs. 3(a)

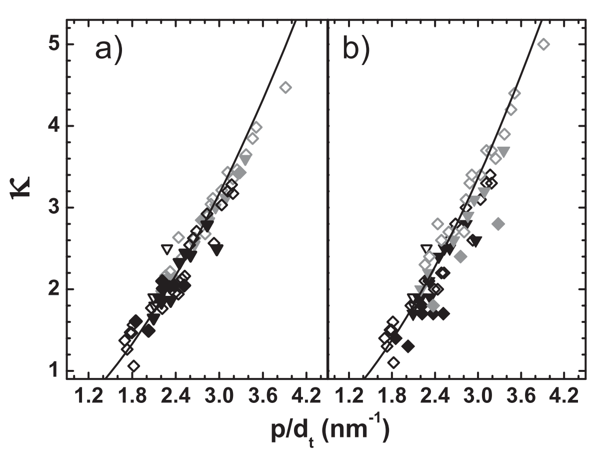

Figure 3 The κ values fitted to the AA and SG E_{33}^S and E_{44}^S transitions. Parts (a) and (b) show, respectively, results for κ when the chirality correction is taken into account and when its not. The solid gray/black diamonds stand for the AA/SG E_{33}^S type I transitions, the open gray/black diamonds stand for the AA/SG E_{33}^S type II, the solid gray/black down-triangles stand for the AA/SG E_{44}^S type I and the open black down-triangle stand for the SG E_{44}^S type II. In (a) the black curve is obtained by fitting the data with Eq. (2) and the curve in (b) is given by Eq. (1).

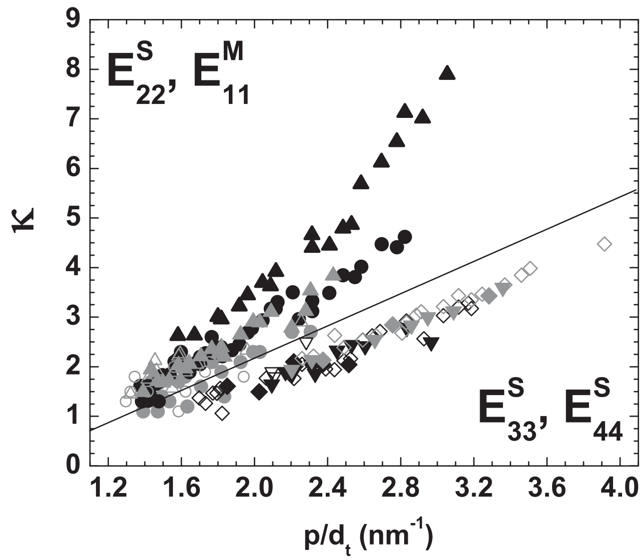

Figure 4 The chiral angle corrected κ values for higher and lower transitions of both AA and SG SWNTs are merged into an unique plot κ *versus* d_t, thus giving a general picture of the dielectric screening problem. The legend for the symbols is the same as used previously in the other figures. The black solid line is just a guide to the eyes showing a clear brake between higher and lower energy transitions.

and (b) show, respectively, the κ values when the chirality correction is and is not taken into account. In this case, one can visibly see that the chirality correction slightly improves the data. It is interesting to note that the chirality correction, in fact, decreases only the spread around the fitting curve [black solid line in Fig. 3(a)]. Then it confirms that C_κ does not change from 0.49, in agreement with the value given by Ref. [23].

In Fig. 4 the chiral angle corrected κ values for higher and lower transitions of both the AA and SG SWNTs are merged into one unique κ *versus* d_t plot, giving a general picture of the dielectric screening problem. It is clear that two regimes still exist, one for the lower and another for the higher energy transitions (besides, of course, the natural separation due to different κ_{env}). However, this is an indication that something more fundamental is needed to properly explain the screening behavior of κ. This problem has been addressed in [28].

4 Conclusions In summary, we have shown that although the biggest dependence of the dielectric constant κ for describing the dielectric energy transitions screening comes from the SWNT diameter, the accuracy in κ can be improved by simply considering a term accounting for the chiral angle correction in the relation between κ and d_t, as given by Eq. (2). The chiral angle corrected κ for the higher transitions (E_{33}^S, E_{44}^S) of both AA and SG samples slightly improves the screening treatment. However, for the lower transitions (E_{22}^S, E_{11}^M) the κ values describing the metallic transitions no longer follow the same curve as for the semiconducting transitions. This can be first understood because of the additional screening offered by free-carriers in metallic systems. If the exciton size (l_κ) is taken into account, all κ values (fitting both higher and lower transitions) for a given sample, collapse into a unique κ *versus* d_t curve [28].

Acknowledgements P.T.A. and A.J. acknowledge MCT-CNPq and the AFOSR/SOARD Project (Award no. FA9550-08-1-0236). ARTN acknowledges financial support from MEXT scholarship. R.S. and K.S. acknowledge MEXT Grant no. 20241023. M.S.D. acknowledges NSF Grant no. DMR-07-04197.

References

[1] C. Dekker, Phys. Today **52**, 22 (1999).
[2] A. Javey, Nature **424**, 654 (2003).
[3] M. S. Dresselhaus, G. Dresselhaus, R. Saito, and A. Jorio, Phys. Rep. **409**, 47 (2005).
[4] A. Jorio, M. S. Dresselhaus, and G. Dresselhaus, Carbon Nanotubes: Advanced Topics in the Synthesis, Structure, Properties and Applications, Vol. 111, Springer Ser. Top. Appl. Phys. (Springer-Verlag, Berlin, 2008).
[5] C. L. Kane and E. J. Mele, Phys. Rev. Lett. **90**, 207401 (2003).
[6] K. Sato, R. Saito, J. Jiang, G. Dresselhaus, and M. S. Dresselhaus, Phys. Rev. B **76**, 195446 (2007).
[7] J. Jiang, R. Saito, Ge. G. Samsonidze, A. Jorio, S. G. Chou, G. Dresselhaus, and M. S. Dresselhaus, Phys. Rev. B **75**, 035407 (2007).
[8] V. N. Popov, New J. Phys. **6**, 17 (2004).
[9] V. N. Popov and L. Henrard, Phys. Rev. B **70**, 115407 (2004).
[10] Ge. G. Samsonidze, R. Saito, N. Kobayashi, A. Grüneis, J. Jiang, A. Jorio, S. G. Chou, G. Dresselhaus, and M. S. Dresselhaus, Appl. Phys. Lett. **85**, 5703 (2004).
[11] C. D. Spataru, S. Ismail-Beigi, L. X. Benedict, and S. G. Louie, Phys. Rev. Lett. **92**, 077402 (2004).
[12] C. L. Kane and E. J. Mele, Phys. Rev. Lett. **93**, 197402 (2004).
[13] P. T. Araujo, S. K. Doorn, S. Kilina, S. Tretiak, E. Einarsson, S. Maruyama, H. Chacham, M. A. Pimenta, and A. Jorio, Phys. Rev. Lett. **98**, 067401 (2007).
[14] T. Michel, M. Paillet, J. C. Meyer, V. N. Popov, L. Henrard, and J.-L. Sauvajol, Phys. Rev. B **75**, 155432 (2007).
[15] S. M. Bachilo, M. S. Strano, C. Kittrell, R. H. Hauge, R. E. Smalley, and R. B. Weisman, Science **298**, 2361 (2002).
[16] M. Strano, S. K. Doorn, E. H. Haroz, C. Kittrell, R. H. Hauge, and R. E. Smalley, Nano Lett. **3**, 1091 (2003).
[17] H. Telg, J. Maultzsch, S. Reich, F. Hennrich, and C. Thomsen, Phys. Rev. Lett. **93**, 177401 (2004).
[18] C. Fantini, A. Jorio, M. Souza, M. S. Strano, M. S. Dresselhaus, and M. A. Pimenta, Phys. Rev. Lett. **93**, 147406 (2004).
[19] M. Y. Sfeir, T. Beetz, F. Wang, L. Huang, X. M. H. Huang, M. Huang, J. Hone, S. O'Brien, J. A. Misewich, T. F. Heinz, Wu. Lijun, Yimei Zhu, and L. E. Brus, Science **312**, 554 (2006).
[20] P. T. Araujo, I. O. Maciel, P. B. C. Pesce, M. A. Pimenta, S. K. Doorn, H. Qian, A. Hartschuh, M. Steiner, L. Grigorian, K. Hata, and A. Jorio, Phys. Rev. B **77**, 241403(R) (2008).
[21] P. T. Araujo, C. Fantini, M. M. Lucchese, M. S. Dresselhaus, and A. Jorio, Appl. Phys. Lett. **95**, 261902 (2009).
[22] P. T. Araujo, P. B. C. Pesce, M. S. Dresselhaus, K. Sato, R. Saito, and A. Jorio, Phys. E **42**, 1251 (2010).
[23] P. T. Araujo, A. Jorio, M. S. Dresselhaus, K. Sato, and R. Saito, Phys. Rev. Lett. **103**, 146802 (2009).
[24] Y. Miyauchi, R. Saito, K. Sato, Y. Ohno, S. Iwasaki, T. Mizutani, J. Jiang, and S. Maruyama, Chem. Phys. Lett. **442**, 394 (2007).
[25] T. Ando, J. Phys. Soc. Jpn. **66**, 1066 (1997).
[26] V. Perebeinos, J. Tersoff, and Ph. Avouris, Phys. Rev. Lett. **92**, 257402 (2004).
[27] R. Saito, G. Dresselhas, and M. S. Dresselhaus, Phys. Rev. B **61**, 2981 (2000).
[28] A. R. T. Nugraha, R. Saito, K. Sato, P. T. Araujo, A. Jorio, and M. S. Dresselhaus, Appl. Phys. Lett., accepted.